

Spatial coexistence of synchronized oscillation and death: A chimeralike state

Partha Sharathi Dutta ^{*}

Department of Mathematics, Indian Institute of Technology Ropar, Rupnagar 140 001, Punjab, India

Tanmoy Banerjee [†]

Department of Physics, University of Burdwan, Burdwan 713 104, West Bengal, India

(Received 5 June 2015; revised manuscript received 25 August 2015; published 22 October 2015)

We report an interesting spatiotemporal state, namely the chimeralike incongruous coexistence of *synchronized oscillation* and *stable steady state* (CSOD) in a network of nonlocally coupled oscillators. Unlike the *chimera* and *chimera death* state, in the CSOD state identical oscillators are self-organized into two coexisting spatially separated domains: In one domain neighboring oscillators show synchronized oscillation and in another domain the neighboring oscillators randomly populate either a synchronized oscillating state or a stable steady state (we call it a death state). We consider a realistic ecological network and show that the interplay of nonlocality and coupling strength results in two routes to the CSOD state: One is from a coexisting mixed state of amplitude chimera and death, and another one is from a globally synchronized state. We provide a qualitative explanation of the origin of this state. We further explore the importance of this study in ecology that gives insight into the relationship between spatial synchrony and global extinction of species. We believe this study will improve our understanding of chimera and chimeralike states.

DOI: 10.1103/PhysRevE.92.042919

PACS number(s): 05.45.Xt, 05.65.+b, 87.23.Cc

Understanding of collective dynamical behaviors in networks of coupled oscillators has been an active area of extensive research in the fields of physics, chemistry, biology, engineering, and social sciences. Coupled oscillators show a plethora of cooperative phenomena, such as synchronization [1], amplitude death [2], oscillation death [3], chimera [4], chimera death [5], etc. Two intriguing spatiotemporal dynamical states, namely the *chimera* and the recently observed *chimera death*, have been in the center of recent research on coupled oscillators for their rich complex behaviors.

The chimera state is a fascinating spatiotemporal state where synchronous and asynchronous oscillations coexist in a network of coupled identical oscillators. After its discovery by Kuramoto and Battogtokh [6] and mathematical proof in Ref. [7], the chimera state attracted immediate attention because of its possible connection with *unihemispheric sleep* in certain species [4], the multiple time scales of sleep dynamics [8], etc. Unlike phase chimera, where chimera occurs in the phase part, recently it is found that in the strong coupling limit amplitude effects come into play that result in amplitude-mediated chimera [9] and amplitude chimera [5,10]; in the amplitude chimera state the coexistence of synchrony and asynchrony appears only in the amplitude part. The existence of chimera has also been established in many experiments, e.g., in optical systems [11], chemical oscillators [12], mechanical systems [13], and electronic systems [14]. Further, chimera states have been observed in various fields; examples include [15] the FitzHugh-Nagumo oscillator, the SNIPER model of excitability of type I, and autonomous Boolean networks (for an elaborate review, please see Ref. [4]). Recently, a chimera state in population dynamics was observed using the lattice limit cycle (LLC) model [16].

On the other hand, the *chimera death* (CD) state was discovered very recently by Zakharova *et al.* [5] in a network of Stuart-Landau oscillators under nonlocal coupling. The CD state connects the chimera state to the oscillation death (OD) state [17,18]. In the OD state oscillators populate different branches of a stable inhomogeneous steady state (IHSS) [3,17–19]. According to Ref. [5], in the *chimera death* state the population of oscillators in a network splits into coexisting domains of spatially coherent OD (where neighboring nodes attain essentially the same branch of the IHSS) and spatially incoherent OD (where the neighboring nodes jump among the different branches of IHSS in a completely random manner). Later, CD is also found in a network of mean-field diffusively coupled oscillators [20].

In summary, the *chimera* state is a spatial coexistence of coherent and incoherent oscillations, and the *chimera death* state is a spatial coexistence of coherent and incoherent branches of oscillation death state. Thus, the next natural question arises: Is it possible to have an emergent state in a network of oscillators that shows a chimeralike coexistence of coherent oscillation and stable steady state?

In this paper, we find the answer in the affirmative. Here, we show that in a realistic ecological network consists of Rosenzweig-MacArthur oscillators [21] under nonlocal coupling topology, the interplay of nonlocality and coupling strength gives rise to an interesting spatiotemporal state. In this state, the population of oscillators split into two coexisting, distinct, spatially separated domains: In one domain oscillators are oscillating in synchrony (i.e., coherently), and in another domain neighboring oscillators depict spatially synchronized oscillation and stable steady state in a random manner (i.e., incoherently). Hereafter, we call this state a *chimeralike synchronized oscillation and death* (CSOD) state (the stable steady state is denoted as a *death* state). Depending upon the coupling range and coupling strength, we identify two types of transitions to the CSOD state: With increasing coupling range (for a moderate coupling strength) the CSOD state arises from

^{*}parthasharathi@iitrpr.ac.in

[†]Corresponding author: tbanerjee@phys.buruniv.ac.in

a coexisting mixed state of amplitude chimera and death state; on the other hand, for an increasing coupling strength (with a moderate coupling range) the CSOD state comes from a globally synchronized oscillation state. However, in both the cases, under large coupling range and strength, the CSOD state is transformed into a chimera death state. Thus, the CSOD state bridges the gap between the amplitude chimera and the chimera death state. We further discuss the ecological importance of this emergent behavior that gives us insight into the relationship between spatial synchrony and global extinction of species, which are thought of as closely connected phenomena in ecology [22]: Spatial synchrony may lead to global extinction of species. Here we show that our results differ from this general consensus, and local extinction of a species does not necessarily lead to a global extinction of that species.

Here we consider the following network of N identical nonlocally coupled Rosenzweig-MacArthur (RM) oscillators:

$$\frac{dV_i}{dt} = rV_i \left(1 - \frac{V_i}{K}\right) - \frac{\alpha V_i}{V_i + B} H_i, \quad (1a)$$

$$\frac{dH_i}{dt} = H_i \left(\frac{\alpha\beta V_i}{V_i + B} - m\right) + \frac{\sigma}{2P} \sum_{k=i-P}^{i+P} (H_k - H_i), \quad (1b)$$

with V and H , respectively, representing vegetation and herbivore density, interacting in $i (= 1, 2, \dots, N)$ discrete patches (or nodes) (i is taken as modulo N). The local dynamics in each node are governed by the following system parameters: r is the intrinsic growth rate, K is the carrying capacity, α is the maximum predation rate of the herbivore, B is the half-saturation constant, β represents the herbivore efficiency, and m is the mortality rate of the herbivore. Interaction between nodes is governed by two coupling parameters: σ is the coupling strength and P controls the coupling range, where $1 \leq P \leq \frac{N}{2}$. Two limiting values of P , i.e., $P = 1$ and $P = N/2$, represent local and global coupling, respectively. This nonlocal coupling topology has been used to observe chimera [10] and chimera death state [5] in generic oscillators and maps. In spatial ecology, herbivores generally move up to certain farthest neighbors to get resources, as they have some limitations in spatial movements; thus this nonlocal coupling represents a more realistic situation in ecology in comparison with global coupling [24]. Each node is described by the Rosenzweig-MacArthur model, the choice of which is led by the fact that it is the simplest model that can actually be applied in *real ecosystems*. As a result, this model becomes a standard spatially structured prey-predator model in theoretical as well as applied ecology [23,24].

An individual RM oscillator [see Eqs. (1) for $\sigma = 0$ and a fixed i] has the following steady states: (i) $(V^*, H^*) = (0, 0)$, where the eigenvalues are $\lambda = r, -m$ and the equilibrium point is a saddle point, (ii) $(V^*, H^*) = (K, 0)$, where the eigenvalues are $\lambda = -r, -m + \alpha\beta \frac{K}{K+B}$ and the equilibrium point is either a stable node or a saddle node, depending upon the values of the parameters, and finally (iii) $(V^*, H^*) = [\frac{mB}{\alpha\beta-m}, \frac{r}{\alpha}(1 - \frac{mB}{K(\alpha\beta-m)})(\frac{\alpha\beta}{\alpha\beta-m})]$, where this nontrivial equilibrium point is stable for parameter values satisfying the inequality $\frac{B}{K} < \frac{(\alpha\beta-m)}{(\alpha\beta+m)}$. Beyond a certain K , this equilibrium point becomes

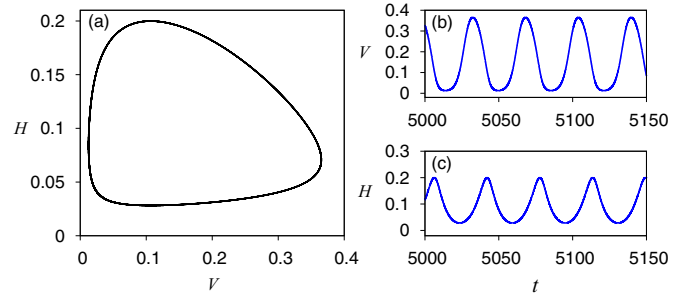


FIG. 1. (Color online) (a) Limit cycle attractor and (b), (c) time series of the uncoupled Rosenzweig-MacArthur model given by Eqs. (1) for $r = 0.5$, $K = 0.5$, $\alpha = 1$, $B = 0.16$, $\beta = 0.5$, and $m = 0.2$.

unstable and gives rise to a stable limit cycle through Hopf bifurcation. In general, further increase in K gradually increases amplitude of the limit cycle, thus bringing the density of either the prey or the predator or both the populations closer to zero, eventually leading to the extinction of the ecosystem; this is known as “the paradox of enrichment” [25] proposed by Rosenzweig in 1971. A subsequent realistic range [26] of K is 0.15 to 3 and range of m is 0.03 to 0.41. In Fig. 1, a stable limit cycle is shown for the following parameter values, which are based on experimental data reported in Ref. [26]: $r = 0.5$, $K = 0.5$, $\alpha = 1$, $B = 0.16$, $\beta = 0.5$, and $m = 0.2$.

To explore various spatiotemporal patterns in the network, we take $N = 100$ and integrate Eqs. (1) numerically [27]. While presenting the simulation results, a large amount of initial integration time ($t = 5000$) is discarded in order to ensure the steady-state behavior. At first, we consider a moderate coupling strength, $\sigma = 1.7$, and increase the coupling range, $\gamma = P/N$, from a lower value. For lower coupling range ($\gamma \leq 0.05$) we observe a mixed state comprised of amplitude chimera and stable zero steady state (i.e., death state). This is shown in Figs. 2(a) and 2(b) for $\gamma = 0.01$ and $\gamma = 0.03$, respectively. The left panel in Fig. 2 shows the space-time color map of V_i and the right panel shows snapshots of V_i in the steady state with oscillator index (i). The shaded regions in Figs. 2(a) and 2(b) (right panel) show this mixed state of amplitude chimera and death: The amplitude chimera interrupted by death state is an interesting observation in the context of coupled oscillators. Further increase in coupling range γ results in the CSOD state where the population of oscillators splits into two distinct coexisting domains: In one domain the neighboring nodes oscillate in synchrony while in another domain the neighboring nodes randomly populate either the synchronized oscillating state or the stable steady (death) state. This spatiotemporal state is shown in Fig. 2(c) for $\gamma = 0.2$ (i.e., $P = 20$). Here we see that in the shaded region [right panel of Fig. 2(c)] the neighboring oscillators populate either synchronized oscillation state or stable zero steady state in a random sequence. However, in the nonshaded region only synchronized oscillation exists except in the rightmost nodes where few oscillators attain the death state. This chimera-like spatiotemporal state is interesting because here the stable steady state coexists with synchronized oscillations, which is unlike the chimera state or chimera death state. We also verify that this CSOD state is preserved for a larger number of

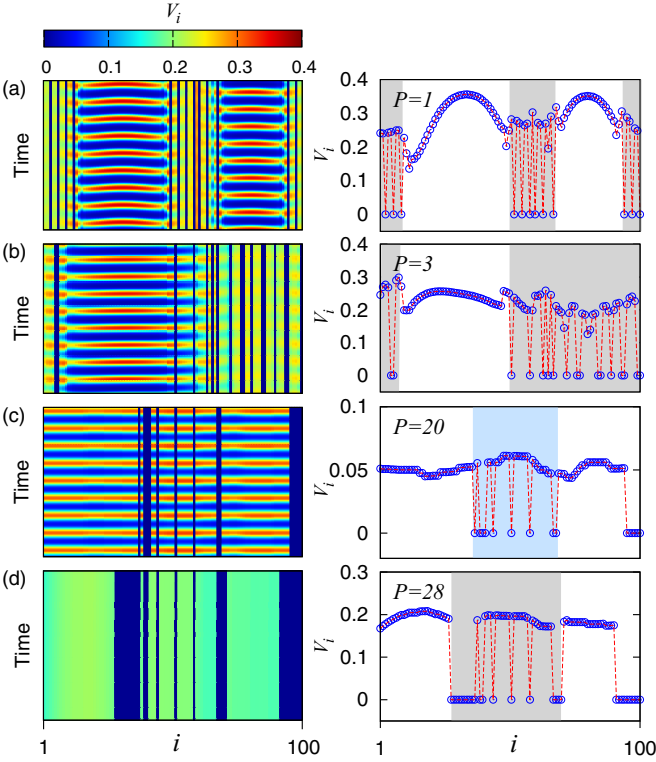


FIG. 2. (Color online) Left panel: Spatiotemporal color map and right panel: Snapshot of V_i (at $t = 5900$) with oscillator index i [red (dotted) line is for visual guidance]. Coupling strength $\sigma = 1.7$, $N = 100$. (a) $P = 1$ ($\gamma = 0.01$) and (b) $P = 3$ ($\gamma = 0.03$) show the mixed state of amplitude chimera and stable zero steady state (gray shade in right panels are for visual guidance). (c) $P = 20$ ($\gamma = 0.2$): *Chimera-like synchronized oscillation and death* (CSOD) state. Cyan (gray) shaded region in the right panel shows the random sequential occurrence of the synchronized oscillation and zero steady state of the neighboring nodes. (d) $P = 28$ ($\gamma = 0.28$): The chimera death state. Initial time $t = 5000$ is discarded before presenting the figures. Other parameters are same as used in Fig. 1.

nodes, N (see Appendix A for the CSOD state for $N = 300$). If we further increase the coupling strength, we find the chimera death state [Fig. 2(d) for $\gamma = 0.28$]. We notice that instead of populating *two* branches of OD [5,20], denoted as lower and upper branches, here in the CD state, the OD state has more than two branches [later it is clearly shown in Fig. 8(b)]. The multiple branches (more than two) of OD were reported earlier in Ref. [28] for sixteen *locally* coupled genetic relaxation oscillators, but in a network of large number of oscillators with *nonlocal* coupling it is an important observation (to be discussed later on).

We also identify one more significant route to the CSOD state with increasing coupling strength (σ) and a fixed γ , namely the transition from a global in-phase synchronized oscillating state to the CSOD state. This transition is shown in Figs. 3(a) and 3(b) for $\sigma = 0.5$ and $\sigma = 2.4$, respectively (for $\gamma = 0.1$, i.e., $P = 10$). Here also, the CSOD state is transformed into a multibranch chimera death state for higher coupling strength (not shown).

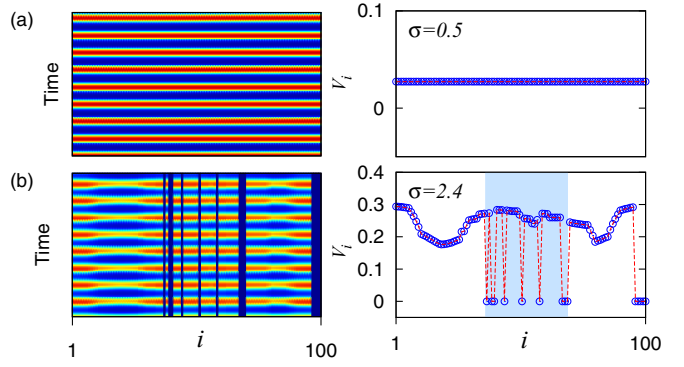


FIG. 3. (Color online) Left panel: Spatiotemporal color map (color bar same as Fig. 2). Right panel: Snapshot of V_i (at $t = 5900$) with oscillator index i . Coupling range $\gamma = 0.1$ (i.e., $P = 10$), $N = 100$. (a) $\sigma = 0.5$: Global in-phase synchronized oscillation. (b) $\sigma = 2.4$: The CSOD state. Cyan (gray) shaded region is for visual guidance of the incoherent region. Other parameters are the same as used in Fig. 1.

At this point, it is also interesting to pay attention to the behavior of the herbivore (H). We notice that when vegetation (V) is in the CSOD state, H is in a *mixed oscillation state* where a subset of populations show a synchronized limit cycle and the remaining subset depicts a random sequential occurrence of larger and relatively smaller amplitude limit cycles. This is physically intuitive from Eqs. (1), which reveal that diffusion occurs to one of the species, i.e., H only; for lower coupling strength and range this diffusion is not strong enough to impose a complete death or stable steady state to H . Thus, at the nodes where V reaches a stable steady state, H reaches an oscillatory state, which is manifested in the form of a relatively smaller amplitude oscillation. This observation is important from ecological perspective too. Since vegetation V cannot move of its own, if V in a certain patch becomes extinct, it stuck to that state. However, significantly, herbivores of that patch can harvest resources from the other patches present in the network and recolonize themselves in order to avoid extinction. However, due to the finite coupling range they only manage to get resources from a limited number of patches, which makes their amplitude smaller. For the stronger coupling strength and larger coupling range, diffusion through nonlocal coupling is sufficient to impose the CD state; i.e., both V and H arrive at the respective steady states. Also, unlike the behavior of V in the amplitude chimera state, we observe a conventional amplitude chimera in the H variable, i.e., in H amplitude chimera is not interrupted by death. These observations are summarized in Fig. 4 for the parameter values used in Fig. 2. Figures 4(a) and 4(b) show the conventional amplitude chimera in H . Figure 4(c) shows the mixed oscillation state in H for $\sigma = 1.7$ and $P = 20$ ($\gamma = 0.2$); we can see that unlike the death states of V in the CSOD state, here H executes an oscillation of relatively smaller amplitude as prominent from the sudden dips in the snapshot of H_i at a certain time. Interestingly, for $\sigma = 1.7$ and $P = 28$ ($\gamma = 0.28$), both V and H are in the chimera death (CD) state.

Next, we quantify the spatiotemporal behavior where synchronized oscillation and stable zero steady (death) state coexist. In order to distinguish between the oscillation and

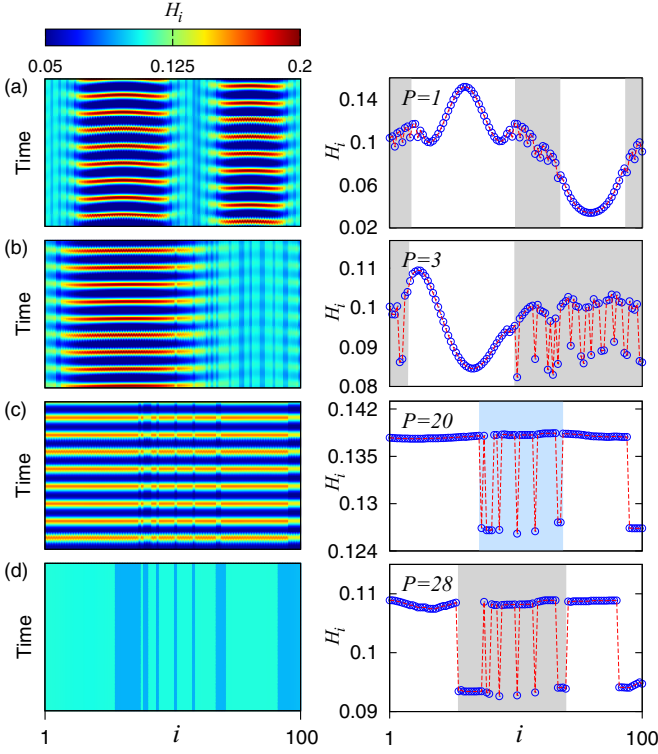


FIG. 4. (Color online) Left panel: Spatiotemporal color map. Right panel: Snapshot of H_i (at $t = 5900$) with oscillator index i . Coupling strength $\sigma = 1.7$, $N = 100$. (a) $P = 1$ ($\gamma = 0.01$) and (b) $P = 3$ ($\gamma = 0.03$) show the amplitude chimera. (c) $P = 20$ ($\gamma = 0.2$): mixed oscillation state. Cyan (gray) shaded region in the right panel shows the random sequential occurrence of two different types of limit cycles in the neighboring nodes. (d) $P = 28$ ($\gamma = 0.28$): The chimera death state. Initial time $t = 5000$ is discarded before presenting the figures. Other parameters are the same as used in Fig. 1.

death, we compute the standard deviation (S.D.) of each node given by

$$\Delta_i = \sqrt{\langle (X_i^2) - \langle X_i \rangle^2 \rangle}, \quad (2)$$

where $X = V, H$. The $\langle \rangle$ signs denote the time average, which is carried out over a long time period ($t = 3000$ in the steady state). For a stable steady state (i.e., a death state) S.D. (Δ_i) must be zero and in the oscillatory condition it will show a finite nonzero value. Figures 5(a) and 5(b) show Δ_i values of the CSOD states shown by V in Figs. 2(c) and 3(b), respectively. For the CSOD state, in the incoherent region, we see that the Δ_i changes from a finite nonzero value to zero in a random manner; in the network where nodes are oscillating in synchrony its value is nonzero and shows a continuous spatial variation. In the case of mixed oscillation state of H , we notice that Δ_i shows a random variation from finite nonzero value to a relatively smaller value in the incoherent region [see Fig. 5(c)]; the dips in Δ_i indicate the oscillations of smaller amplitude. Figure 5(d) shows the Δ_i corresponding to the CD state (of both V and H), indicating that all the nodes reach stable steady states.

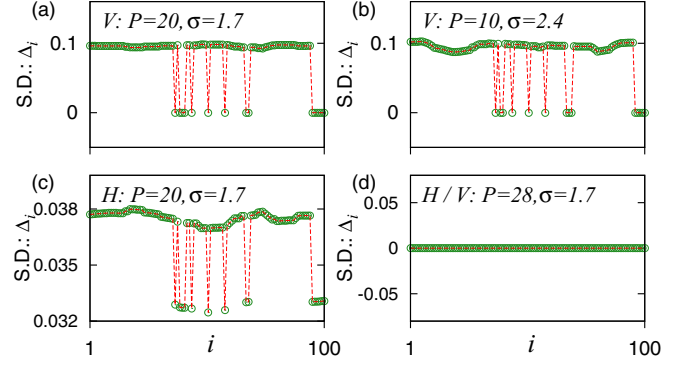


FIG. 5. (Color online) Standard deviation (Δ_i) with index i of (a) the CSOD state of Fig. 2(c), (b) the CSOD state of Fig. 3(b), (c) the mixed oscillation state of H in Fig. 4(c), and (d) CD states of V [Fig. 2(d)] and H [Fig. 4(d)]. Other parameters are the same as used in Fig. 1.

In order to reveal the complete spatiotemporal scenario of the considered network, we rigorously compute the phase diagram in the γ - σ plane (the unsynchronized zone with very small σ value is not shown). From the phase diagram [see Fig. 6] it is clear that the region of occurrence of the CSOD state (and the mixed oscillation state for H) is broad enough. It is seen that beyond $\gamma \approx 0.37$ (i.e., $P \approx 37$) no CSOD occurs; here an increase in σ transforms the synchronized oscillation state (SYNC) directly to the chimera death (both for V and H). Apart from the CSOD state, we make an important observation regarding the CD state; namely, beyond a certain coupling strength (here, $\sigma \approx 3$), we find the CD state even in the local coupling (i.e., $P = 1$) [29]. The CD states in V and H under local coupling ($P = 1$) are shown in Fig. 7 for

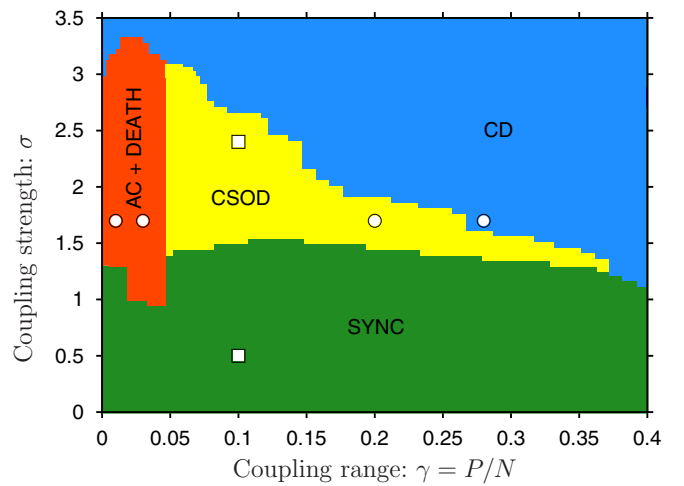


FIG. 6. (Color online) Phase diagram in the γ - σ plane. CSOD: chimeralike synchronized oscillation and stable zero steady state (death); SYNC: global in-phase synchronized oscillation; CD: chimera death; and AC + death: coexistence of amplitude chimera and stable zero steady state. Note that CD occurs even in the local coupling ($P = 1$) beyond $\sigma \approx 3$. The symbols \circ indicate the coupling parameter values used for generating Figs. 2(a)–2(d) and 4(a)–4(d). \square represents the same for generating Figs. 3(a) and 3(b). Other parameters are the same as used in Fig. 1.

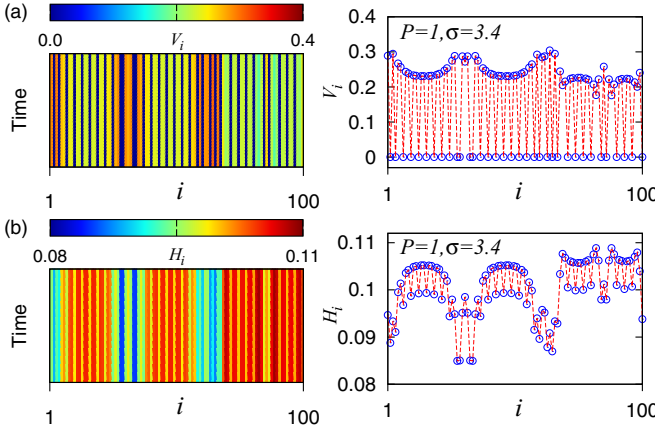


FIG. 7. (Color online) Chimera death in local coupling (i.e., $P = 1$), $\sigma = 3.4$. Left panel: spatiotemporal color map. Right panel: snapshot (at $t = 5900$) with oscillator index i of (a) V_i and (b) H_i . Other parameters are the same as Fig. 1.

an exemplary coupling strength $\sigma = 3.4$; multiple cluster CD state is observed from the figure. In the phase diagram the symbols \circ indicate the coupling parameter values used for generating Figs. 2(a)–2(d) and Figs. 4(a)–4(d), whereas \square represents the same for generating Figs. 3(a) and 3(b). In this context, it should be noted that in the phase diagram the boundaries among different phases are not very sharp; they tend to change with initial conditions. However, we observe that the overall qualitative structure of the phase diagram is preserved for all the initial conditions or number of nodes.

Next, we provide a qualitative explanation of the genesis of the CSOD state. We find that it has a strong connection with the *inhomogeneous limit-cycle* (IHLC) state in a network [18,30]. The IHLC state may be of two types: (i) a state where some nodes are in a stable steady state or quasisteady state with a negligible amplitude [18] while the rest undergo oscillations, or (ii) a state in which all the nodes depict oscillations but two or more subsets of oscillators have their origin shifted in phase space (i.e., the limit cycles are inhomogeneous) [17]. To visualize the scenario, we plot the time series of all the V_i 's [Fig. 8(a)] for an exemplary value of $\gamma = 0.2$ and $\sigma = 1.7$. From Fig. 8(a) we observe that a population of oscillators occupy the trivial zero steady state (i.e., $V = 0$ state), while the rest of the oscillators are in the in-phase synchronized oscillating state [i.e., IHLC of type (i)]. Thus, depending upon judiciously chosen *spatial* initial conditions (see Appendix B), individual nodes may populate either the upper oscillating branch or the lower steady state (i.e., $V = 0$) branch in a random sequence, which results in the CSOD state [as shown in Fig. 2(c)]. Thus, we may conjecture that, apart from the RM oscillator, the CSOD state may occur in systems where this type of IHLC state exists [Fig. 8(a)]. The corresponding time series of H is shown in Fig. 8(c), which shows oscillations shifted in their origin [i.e., IHLC of type (ii)]; this type of IHLC in two coupled Stuart-Landau oscillators has been reported in Ref. [17]. In the case of higher coupling range and strength, e.g., $\gamma = 0.28$ and $\sigma = 1.7$, oscillators populate the

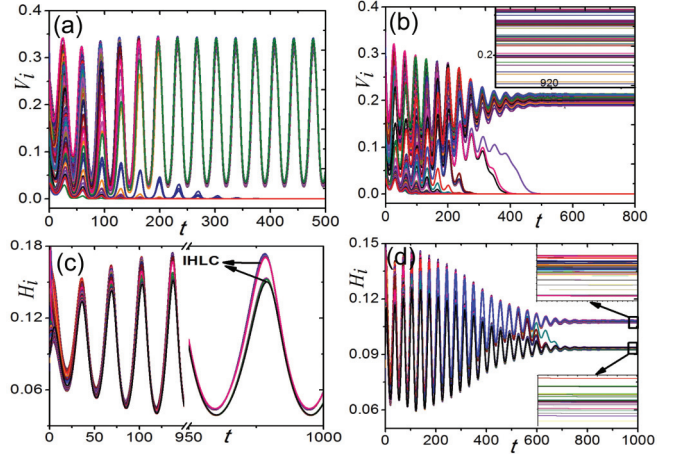


FIG. 8. (Color online) Time series of V_i 's for (a) $\gamma = 0.2$ and $\sigma = 1.7$: synchronized limit-cycle oscillation (upper branch) and stable zero steady state (i.e., $V = 0$) coexists. (b) $\gamma = 0.28$ and $\sigma = 1.7$: temporally stable multibranch OD. The inset shows the multiple branches around $V_i = 0.2$. Panels (c) and (d) show the corresponding time-series of H_i , respectively: (c) IHLC having offset in limit cycles of two subpopulations. (d) Multiple OD branches are seen in both the upper and lower branches. Other parameters are the same as used in Fig. 1.

multibranch OD state [Fig. 8(b), see also the inset]; here a set of proper spatial initial conditions should result in chimera death in the network [as shown in Fig. 2(d)]. Figure 8(d) shows the corresponding time series of H ; it is interesting to note that the upper as well as the lower branches of the oscillation death state are split into several multibranch steady states.

Finally, we discuss the importance of the results in ecology. In spatial ecology nonlocal coupling arises under the assumption that all spatially separated patches (or nodes) are connected only to a certain number of neighboring nodes in a fragmented landscape, which is a more natural coupling scheme than the global coupling. In ecology, it is generally believed that spatial synchrony and global extinction are two strongly correlated phenomena (see for example, Ref. [22]). In contrast to this general belief, in the present study we show that, in nonlocal dispersive coupling, although spatial synchronization gives rise to local extinction of a species in one or more patches (or nodes) [i.e., the *death* state], it defies the *global extinction* of the species (i.e., not all the oscillators go to the *death* state). Moreover, a general consensus in ecology is that spatial synchrony and dispersal-induced stability (or temporal stability) are two conflicting outcomes of dispersion among the population of patches. In the existing studies it is shown that dispersion among identical patches results in spatial synchrony; on the other hand, the combination of spatial heterogeneity and dispersion is necessary for dispersal-induced stability [31]. Here our results show that depending on coupling range and strength, spatial synchronization among *identical* patches (or nodes) leads to temporally stable multibranch (more than two) IHSS and a cluster of them has nonzero steady states. Thus, to achieve temporal stability the patches need not to be heterogeneous

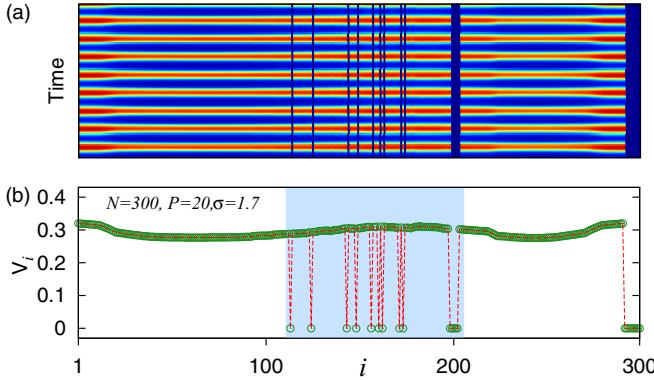


FIG. 9. (Color online) (a) Spatiotemporal color map of V_i and (b) a snapshot of V_i at a fixed time $t = 5900$ [red (dotted) line is for visual guidance]. Number of oscillators $N = 300$, coupling strength $\sigma = 1.7$, and coupling range $P = 20$ ($\gamma = 0.2$): the CSOD state. Cyan (gray) shaded region in panel (b) shows the random sequential occurrence of the synchronized oscillation and zero steady state of the neighboring nodes. Other parameters are the same as used in Fig. 1 of the main article. The color bar is same as Fig. 2 of the main article.

but nonlocal coupling is sufficient. Further, the occurrence of the amplitude chimera interrupted by death is interesting and its proper interpretation in ecology deserves further attention.

In conclusion, in this paper we have reported an important spatiotemporal state, namely the CSOD state, in a realistic ecological network with nonlocal coupling topology. In this state a subset of oscillators populate spatially synchronized oscillation and stable steady state in a random manner, and the rest of the oscillators oscillate in synchrony. This spatiotemporal state is unlike the chimera state (where coherent and incoherent oscillations coexist) and the chimera death state (where neighboring oscillators populate two branches of OD in coherent and incoherent manner). We have shown two coupling-dependent transition routes to this CSOD state. We have qualitatively established the connection of this emergent state with the inhomogeneous limit-cycle state present in the network. We have further reported the occurrence of the chimera death state even in local coupling topology. We have discussed the ecological importance of the CSOD state, which reveals that spatial synchrony does not necessarily lead to global extinction of a species, which is in contrast to the general consensus. We believe that the CSOD state that arises due to *nonlocality* in coupling may arise in a two-dimensional network also as far as the coupling remains nonlocal. Apart from ecology, we further believe that the present study will improve our understanding of other physical networks, e.g., power grid and communication networks, where it is desirable that failure of certain nodes does not lead to a complete blackout or a global system failure [32].

Authors acknowledge the insightful suggestions of the referees that improved the quality of the paper. T.B. acknowledges financial support from SERB, Department of Science and Technology (DST), India (Grant No. SB/FTP/PS-005/2013).

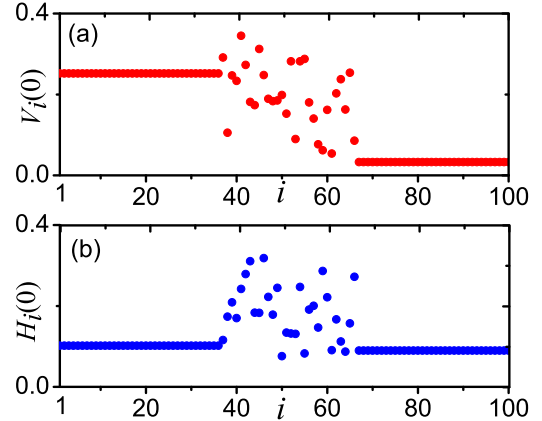


FIG. 10. (Color online) Initial conditions to generate all the results reported in the main text (except Fig. 1). (a) $V_i(0)$ and (b) $H_i(0)$. For detail see the text.

APPENDIX A: CSOD STATE FOR $N = 300$ OSCILLATORS

Spatial coexistence of synchronized oscillation and death (CSOD) state for $N = 300$ oscillators. Figure 9 shows the CSOD state, which ensures that the CSOD state is not due to the finite size effect. One can get the COSD state even in a network consisting of a large number of oscillators.

APPENDIX B: INITIAL CONDITIONS

The initial conditions of each node used in the simulations are shown in Fig. 10 of Appendix B. We assign the following initial conditions: $V_1(0), \dots, V_{36}(0) = 0.252, V_{37}(0), \dots, V_{46}(0) = 0.1 + 0.25\xi, V_{47}(0), \dots, V_{66}(0) = 0.05 + 0.25\xi, V_{67}(0), \dots, V_{100}(0) = 0.033, H_1(0), \dots, H_{36}(0) = 0.102, H_{37}(0), \dots, H_{46}(0) = 0.05 + 0.25\xi, H_{47}(0), \dots, H_{66}(0) = 0.05 + 0.25\xi, H_{67}(0), \dots, H_{100}(0) = 0.09$. Here ξ is a function that gives uniformly distributed random numbers in the range $[0, 1]$ of zero mean. For the first 36 nodes we choose a value around 0.25 because it is half of the half-saturation constant $K = 0.5$, and we observed in Ref. [24] that under a moderate coupling constant (σ) and lower mortality rate (m), the upper value of V resides near 0.25. For the last 34 nodes (i.e., $i = 67, \dots, 100$) we choose a value of V that is near to zero, which is nearer the lower zero value of V . The constant value of H is chosen around 0.1, which is closer to the fixed point of H (see Fig. 1). Apart from these two extreme values of V and H , we choose random initial conditions for the remaining

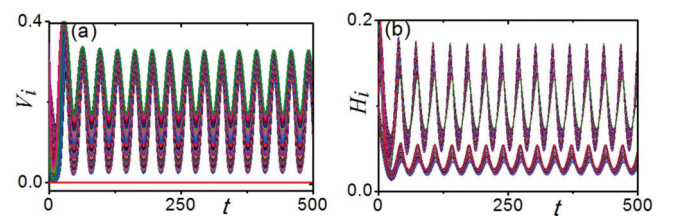


FIG. 11. (Color online) Time series of (a) V_i and (b) H_i . See the text for details.

nodes; we have introduced an offset in order to increase the inhomogeneity among the nodes.

Figure 11 shows the real-time trace of V_i and H_i in the CSOD state with a slight change in initial conditions and a relatively smaller coupling strength $\sigma = 1.5$ (other parameters are the same as used in Fig. 2 of the main text). From Fig. 11(a) we observe that the CSOD state of V_i has multiple (but closely

spaced) oscillating branches along with the zero steady state. Also, now the IHLC state of H_i is more prominent [Fig. 11(b)]; Fig. 11(b) shows that two oscillating branches of H_i (upper and lower) are separated in their origin and also that the lower oscillating branch has a relatively smaller amplitude. We verify that the smaller amplitude oscillations in H_i correspond to the *death* nodes of the CSOD state in V_i .

-
- [1] S. H. Strogatz, *Sync: How Order Emerges from Chaos in the Universe, Nature, and Daily Life* (Hyperion, New York, 2012).
 - [2] G. Saxena, A. Prasad, and R. Ramaswamy, *Phys. Rep.* **521**, 205 (2012).
 - [3] A. Koseska, E. Volkov, and J. Kurths, *Phys. Rep.* **531**, 173 (2013).
 - [4] M. J. Panaggio and D. M. Abrams, *Nonlinearity* **28**, R67 (2015).
 - [5] A. Zakharova, M. Kapeller, and E. Schöll, *Phys. Rev. Lett.* **112**, 154101 (2014).
 - [6] Y. Kuramoto and D. Battogtokh, *Nonlinear Phenom. Complex Syst.* **5**, 380 (2002).
 - [7] D. M. Abrams and S. H. Strogatz, *Phys. Rev. Lett.* **93**, 174102 (2004); D. M. Abrams, R. Mirollo, S. H. Strogatz, and D. A. Wiley, *ibid.* **101**, 084103 (2008).
 - [8] E. Olbrich, J. C. Claussen, and P. Achermann, *Phil. Trans. R. Soc. A* **369**, 3884 (2011).
 - [9] G. C. Sethia and A. Sen, *Phys. Rev. Lett.* **112**, 144101 (2014); G. C. Sethia, A. Sen, and G. L. Johnston, *Phys. Rev. E* **88**, 042917 (2013).
 - [10] I. Omelchenko, Y. Maistrenko, P. Hövel, and E. Schöll, *Phys. Rev. Lett.* **106**, 234102 (2011); I. Omelchenko, B. Riemschneider, P. Hövel, Y. Maistrenko, and E. Schöll, *Phys. Rev. E* **85**, 026212 (2012).
 - [11] A. M. Hagerstrom, T. E. Murphy, R. Roy, P. Hövel, I. Omelchenko, and E. Schöll, *Nat. Phys.* **8**, 658 (2012).
 - [12] M. R. Tinsley, S. Nkomo, and K. Showalter, *Nat. Phys.* **8**, 662 (2012).
 - [13] E. A. Martens, S. Thutupalli, A. Fourrière, and O. Hallatschek, *Proc. Natl. Acad. Sci. USA* **110**, 10563 (2013).
 - [14] L. V. Gambuzza, A. Buscarino, S. Chessari, L. Fortuna, R. Meucci, and M. Frasca, *Phys. Rev. E* **90**, 032905 (2014).
 - [15] I. Omelchenko, O. E. Omelchenko, P. Hövel, and E. Schöll, *Phys. Rev. Lett.* **110**, 224101 (2013); A. Vüllings, J. Hizanidis, I. Omelchenko, and P. Hövel, *New J. Phys.* **16**, 123039 (2014); D. P. Rosin, D. Rontani, N. D. Haynes, E. Schöll, and D. J. Gauthier, *Phys. Rev. E* **90**, 030902(R) (2014).
 - [16] J. Hizanidis, E. Panagakou, I. Omelchenko, E. Schöll, P. Hövel, and A. Provata, *Phys. Rev. E* **92**, 012915 (2015).
 - [17] A. Koseska, E. Volkov, and J. Kurths, *Phys. Rev. Lett.* **111**, 024103 (2013).
 - [18] E. Ullner, A. Zaikin, E. I. Volkov, and J. García-Ojalvo, *Phys. Rev. Lett.* **99**, 148103 (2007).
 - [19] T. Banerjee and D. Ghosh, *Phys. Rev. E* **89**, 052912 (2014); **89**, 062902 (2014); D. Ghosh and T. Banerjee, *ibid.* **90**, 062908 (2014).
 - [20] T. Banerjee, *Europhys. Lett.* **110**, 60003 (2015).
 - [21] M. L. Rosenzweig and R. H. MacArthur, *Am. Nat.* **97**, 209 (1963).
 - [22] M. Heino, V. Kaitala, E. Ranta, and J. Lindström, *Proc. R. Soc. London, Ser. B* **264**, 481 (1997); D. J. D. Earn, P. Rohani, and B. T. Grenfell, *ibid.* **265**, 7 (1998); D. J. D. Earn, S. A. Levin, and P. Rohani, *Science* **290**, 1360 (2000); A. Liebhold, W. D. Koenig, and O. N. Bjornstad, *Annu. Rev. Ecol. Evol. Syst.* **35**, 467 (2004); R. E. Amritkar and G. Rangarajan, *Phys. Rev. Lett.* **96**, 258102 (2006).
 - [23] M. D. Holland and A. Hastings, *Nature (London)* **456**, 792 (2008); E. E. Goldwyn and A. Hastings, *Bull. Math. Biol.* **71**, 130 (2009); *J. Theor. Biol.* **289**, 237 (2011); S. P. Ellner, K. W. Shertzer, and N. G. Hairston Jr., *Science* **290**, 1358 (2000).
 - [24] T. Banerjee, P. S. Dutta, and A. Gupta, *Phys. Rev. E* **91**, 052919 (2015).
 - [25] M. L. Rosenzweig, *Science* **171**, 385 (1971).
 - [26] W. W. Murdoch, R. M. Nisbet, E. McCauley, A. M. deRoos, and W. S. C. Gurney, *Ecology* **79**, 1339 (1998).
 - [27] We use the fourth-order Runge-Kutta algorithm with step size 0.01.
 - [28] A. Koseska and J. Kurths, *Chaos* **20**, 045111 (2010).
 - [29] This point has been suggested by one of the referees.
 - [30] J. Tyson and S. Kauffman, *J. Math. Biol.* **1**, 289 (1975); A. Koseska, E. Ullner, E. I. Volkov, J. Kurths, and J. García-Ojalvo, *J. Theor. Biol.* **263**, 189 (2010).
 - [31] C. J. Briggs and M. F. Hoopes, *Theor. Popul. Biol.* **65**, 299 (2004); K. C. Abbott, *Ecol. Lett.* **14**, 1158 (2011).
 - [32] A. E. Motter, S. A. Myers, M. Anghel, and T. Nishikawa, *Nat. Phys.* **9**, 191 (2013); P. J. Menck, J. Heitzig, J. Kurths, and H. J. Schellnhuber, *Nat. Commun.* **5**, 3969 (2014).